Princeton Plasma Physics Laboratory

PPPL-

PPPL-

PRINCETON
PLASMA PHYSICS
LABORATORY

Princeton Plasma Physics Laboratory
Report Disclaimers

PPPL Report Availability

Princeton Plasma Physics Laboratory:

http://www.pppl.gov/techreports.cfm

Office of Scientific and Technical Information (OSTI):

http://www.osti.gov/bridge

Related Links:

U.S. Department of Energy

Office of Scientific and Technical Information

Fusion Links

Canonicalization and symplectic simulation of the gyrocenter dynamics in time-independent magnetic fields

Ruili Zhang,[1] Jian Liu,[2, *] Yifa Tang,[1] Hong Qin,[2, 3] Jianyuan Xiao,[2] and Beibei Zhu[1]

[1]*LSEC, ICMSEC, Academy of Mathematics and Systems Science,*
Chinese Academy of Sciences, Beijing 100190, China

[2]*Department of Modern Physics and Collaborative Innovation*
Center for Advanced Fusion Energy and Plasma Sciences,
University of Science and Technology of China, Hefei, Anhui 230026, China

[3]*Plasma Physics Laboratory, Princeton University,*
Princeton, New Jersey 08543, USA

Abstract

The gyrocenter dynamics of charged particles in time-independent magnetic fields is a non-canonical Hamiltonian system. The canonical description of the gyrocenter has both theoretical and practical importance. We provide a general procedure of the gyrocenter canonicalization, which is expressed by the series of a small variable ϵ depending only on the parallel velocity u and can be expressed in a recursive manner. We prove that the truncation of the series to any given order generates a set of exact canonical coordinates for a system, whose Lagrangian approximates to that of the original gyrocenter system in the same order. If flux surfaces exist for the magnetic field, the series stops simply at the second order and an exact canonical form of the gyrocenter system is obtained. With the canonicalization schemes, the canonical symplectic simulation of gyrocenter dynamics is realized for the first time. The canonical symplectic algorithm has the advantage of good conservation properties and long-term numerical accuracy, while avoiding numerical instability. It is worth mentioning that explicitly expressing the canonical Hamiltonian in new coordinates is usually difficult and impractical. We give an iteration procedure that is easy to implement in the original coordinates associated with the coordinate transformation. This is crucial for modern large-scale simulation studies in plasma physics. The dynamics of gyrocenters in the dipole magnetic field and in the toroidal geometry are simulated using the canonical symplectic algorithm by comparison with the higher-order non symplectic Runge-Kutta scheme. The overwhelming superiorities of the symplectic method for the gyrocenter system are evidently exhibited.

---

* jliuphy@ustc.edu.cn

I. INTRODUCTION

The dynamics of charged particles in magnetized plasmas consists of the fast gyromotion and the slow guiding center motion. To deal with low frequency phenomena, the gyrokinetic theory has been developed to resolve the multi-scale problem by averaging out or separating the fast gyromotion from the slow gyrocenter motion[1–3]. Gyrokineics provides powerful analytical tools and effective simulation models for the study of magnetized plasmas[1–15]. The gyrocenter system, rooting from the gyro-symmetry, are usually represented by non-canonical gyrocenter coordinates. Its canonicalization can benefit the fundamental theory as well as the advanced simulation techniques. In this paper, we provide a general procedure of constructing canonical coordinates for the gyrocenter dynamics in time-independent electro-magnetic fields in a series form. The canonical coordinates thus can be achieved recursively, without solving the differential equations as in the standard proof of Darboux's theorem. We prove that the truncation of this series to any given order can lead to an exact canonical form for a system, while the Lagrangian of this system approximates to that of the original gyrocenter system in the same order of the truncation. Moreover, if the magnetic field has flux surfaces, the series terminates naturally at the second order and a set of exact canonical coordinates of the gyrocenter system can be obtained directly. This canonicalization scheme can be applied to symplectic simulation of gyrocenter dynamics conveniently. We design the symplectic algorithm for gyrocenter system for the first time, on the basis of the canonicalization. We simulated the gyrocenter dynamics in a dipole magnetic field and a toroidal configuration using the canonical symplectic algorithm and a higher-order Runge-Kutta method for comparison. The long-term conservation properties, numerical accuracy, and numerical stability of canonical symplectic simulation for gyrocenter systems are amply demonstrated in the study.

The symplectic method is a well-known numerical integrator with global conservation properties for canonical Hamiltonian system. It has been successfully applied to test particle simulation and even the PIC method in the study of plasma physics[16]. The standard symplectic scheme requires a canonical structure of the dynamical system. Unfortunately, because the gyrocenter coordinates are non-canonical, the symplectic simulation for gyrocenter system is beset with difficulties. Recently, many efforts have been devoted to the symplectic simulation of gyrocenter dynamics. One plan is to make use of the variation-

al symplectic scheme[17–19]. However, because of its multi-step nature, the variational symplectic algorithm for gyrocenter dynamics sometimes process unexpected numerical instability. An alternative approach is to develop a general and practical procedure of the canonicalization of the gyrocenter system. Then the standard canonical symplectic scheme for gyrocenter dynamics can be applied. According to Darboux's theorem, local canonical coordinates can be theoretically found through solving differential equations. For the gyrocenter dynamics in magnetic fields, several attempts have been made to find the canonical coordinates. Meiss and Hazeltine discussed the existence of the canonical coordinates of the gyrocenter systems, but their canonical scheme is impractical for numerical simulations[20]. White, Zakharov [21] and Gao [22] studied the canonical form of the gyrocenter motion in magnetic fields with toroidal flux-surfaces in detail. Different from the previous methods, we provide a set of direct formulae in which the coordinate transformation is expressed by the series of a small quantity ϵ, which depends on the parallel velocity u, and achieved in a recursive manner. In the process, only matrix multiplication is required, instead of solving differential equations. For numerical calculations, the manipulation of matrices is much more effective than solving differential equations. Furthermore, there is no assumption on properties of the magnetic fields in this canonicalization scheme. Because the series is formally infinite, it should be truncated to contain only finite terms when applying to a specific magnetic configuration. However, the truncated system still preserve good lagrangian structure. We prove that the truncation of the series to any given order generates a set of exact canonical coordinates for the system, whose Lagrangian approximates to that of the original gyrocenter system to the same order of the truncation.

Commonly, the equilibrium magnetic fields we dealt with in plasma physics are not chaotic. This kind of magnetic fields form flux surfaces, i.e., there exists a scalar function Ψ such that $B \cdot \nabla \Psi = 0$. With this assumption, the series form of canonicalization naturally terminates at the second order. So the exact canonical coordinates of the gyrocenter system in a magnetic with flux surfaces can be obtained conveniently. In this case, the canonicalization of the gyrocenter system and the canonical symplectic simulation of gyrocenter dynamics can be achieved without any approximation.

Once the canonical coordinates of the gyrocenter system are obtained, we can apply standard canonical symplectic methods to the study of gyrocenter dynamics. The symplectic Runge-Kutta methods are a class of broadly used symplectic implicit methods. When they

are applied to the canonicalized gyrocenter systems, the problem of expressing the Hamiltonian function in new coordinates is revealed. That's because generally speaking, unless in some special cases, the inverse of this coordinates transformation and hence the new Hamiltonian are quite difficult to express. Here, we give a convenient iteration for numerical computing with original coordinates, in which the calculation of the gradient of the new Hamiltonian is avoided. Then the canonical symplectic simulation of gyrocenter dynamics can be realized.

To verify the correctness of the canonicalization and the advantage of the canonical symplectic simulation, the numerical examples of gyrocenter dynamics in the magnetic fields with dipole and toroidal configuration are carried out. We apply the mid-point rule (a 2nd-order symplectic Runge-Kutta method) to simulate the particle's motion, while observing the evolution of the energy of the gyrocenter systems. The numerical results form the canonical symplectic method have better accuracy and conservation properties than that from the implicit Runge-Kutta method of order 3 applied directly to the non-canonical gyrocenter system in long-term simulation. The canonicalization procedure developed here can be applied to modern large-scale gyrokinetic simulation in both space plasmas and fusion plasmas, where the long-term accuracy and fidelity of algorithms are critical.

The paper is organized as follows. In Sec. II, we discuss the canonicalization of the gyrocenter system in the series form in general. The truncations of the series are also investigated. In Sec. III, we discuss the exact canonical scheme for magnetic fields with flux surfaces. In Sec. IV, we focus on how to construct the canonical symplectic method of the gyrocenter system. Then in Sec. V, numerical examples of gyrocenter dynamics using canonical symplectic algorithms are given. By comparison with the higher-order non-symplectic Runge-Kutta method, the correctness and advantage of the canonicalization and symplectic scheme of the gyrocenter dynamics are verified. Finally in Sec. VI, we give a brief summary and future plan on this topic.

II.   THE CANONICALIZATION OF GYROCENTER DYNAMICS

In this section, we discuss how to canonicalize the gyrocenter system in general. The Lagrangian of the gyrocenter system can be written as[2]

$$L(\mathbf{X}, \dot{\mathbf{X}}, u, \dot{u}) = [\mathbf{A}(\mathbf{X}) + u\mathbf{b}(\mathbf{X})] \cdot \dot{\mathbf{X}} - [\frac{1}{2}u^2 + \mu B(\mathbf{X}) + \phi(\mathbf{X})], \qquad (1)$$

where $\mathbf{B} = \nabla \times \mathbf{A}$ is the magnetic field, $\mathbf{b} = \mathbf{B}/B(\mathbf{X}) = (b_1, b_2, b_3)^\top$ is the unit vector along the direction of magnetic field, $\mathbf{X}$ and u are the position coordinates of the gyrocenter and parallel velocity respectively, and μ is the magnetic moment, which is an adiabatic invariant. $\mathbf{A} = (A_1, A_2, A_3)^\top$ is the vector potential normalized by cm/e, and ϕ is the scalar potential normalized by m/e. The electromagnetic field is assumed to be time-independent in Eq. (1). The Euler-Lagrange equations of L with respect to $\mathbf{X} = (x, y, z)^\top$ and u give the gyrocenter motion equation

$$K(\mathbf{v})\dot{\mathbf{v}} = \nabla H(\mathbf{v}) \tag{2}$$

where $\mathbf{v} = (\mathbf{X}^\top, u)^\top$, $H(\mathbf{v}) = \frac{1}{2}u^2 + \mu B(\mathbf{X}) + \phi(\mathbf{X})$ and $K(\mathbf{v})$ is an antisymmetric matrix

$$K(\mathbf{v}) = \begin{pmatrix} 0 & a_{12} & a_{13} & -b_1 \\ -a_{12} & 0 & a_{23} & -b_2 \\ -a_{13} & -a_{23} & 0 & -b_3 \\ b_1 & b_2 & b_3 & 0 \end{pmatrix}, \tag{3}$$

$$a_{12} = \left(\frac{\partial A_2}{\partial x} - \frac{\partial A_1}{\partial y}\right) + u\left(\frac{\partial b_2}{\partial x} - \frac{\partial b_1}{\partial y}\right),$$
$$a_{13} = \left(\frac{\partial A_3}{\partial x} - \frac{\partial A_1}{\partial z}\right) + u\left(\frac{\partial b_3}{\partial x} - \frac{\partial b_1}{\partial z}\right),$$
$$a_{23} = \left(\frac{\partial A_3}{\partial y} - \frac{\partial A_2}{\partial z}\right) + u\left(\frac{\partial b_3}{\partial y} - \frac{\partial b_2}{\partial z}\right).$$

In the gyrocenter motion equations, the determinant of the matrix K is

$$\det(K(\mathbf{v})) = |\mathbf{b} \cdot \nabla \times (\mathbf{A} + u\mathbf{b})|^2.$$

If the condition $\det(K(\mathbf{v})) \neq 0$ holds, Eq. (2) can be written as a general Hamiltonian system

$$\dot{\mathbf{v}} = K(\mathbf{v})^{-1}\nabla H(\mathbf{v}). \tag{4}$$

The system Eq. (4) is a non-canonical Hamiltonian system. At the same time, a canonical Hamiltonian system, which we struggle to seek, should take the form of

$$\dot{\mathbf{Z}} = J^{-1}\nabla H(\mathbf{Z}), \quad J = \begin{pmatrix} 0 & I_n \\ -I_n & 0 \end{pmatrix}, \tag{5}$$

6

where $\mathbf{Z} \in \mathbb{R}^{2n}$. According to Darboux's theorem, for a non-canonical Hamiltonian system we can find theoretically the local canonical coordinates by solving differential equations, which is an uneconomic method for numerical purpose. To avoid solving differential equations, we don't follow the steps given in the standard proof of Darboux' theorem. Instead, we explore another procedure to realize the canonicalization of the gyrocenter system. Let $\mathbf{Z} = \Phi(\mathbf{v})$ be a transformation from $\mathbb{R}^4$ to $\mathbb{R}^4$, according to the chain rule, Eq. (4) can be written as

$$\dot{\mathbf{Z}} = (\frac{\partial \Phi}{\partial \mathbf{v}}) K(\mathbf{v})^{-1} (\frac{\partial \Phi}{\partial \mathbf{v}})^\top \nabla \tilde{H}(\mathbf{Z}) \tag{6}$$

where $\tilde{H}(\mathbf{Z}) = H(\mathbf{v})$. If we demand $(\frac{\partial \Phi}{\partial \mathbf{v}}) K(\mathbf{v})^{-1} (\frac{\partial \Phi}{\partial \mathbf{v}})^\top = J^{-1}$, i.e., $K(\mathbf{v}) = (\frac{\partial \Phi}{\partial \mathbf{v}})^\top J(\frac{\partial \Phi}{\partial \mathbf{v}})$, Eq. (6) becomes a canonical Hamiltonian system in new coordinates $\mathbf{Z}$ through this transformation. Denoting $\Phi : x \mapsto p_1(\mathbf{v}), y \mapsto p_2(\mathbf{v}), z \mapsto q_1(\mathbf{v}), u \mapsto q_2(\mathbf{v})$, we find the coordinates transformation Φ should satisfy the following conditions:

$$
\begin{aligned}
(\frac{\partial p_1}{\partial x}\frac{\partial q_1}{\partial y} - \frac{\partial q_1}{\partial x}\frac{\partial p_1}{\partial y}) + (\frac{\partial p_2}{\partial x}\frac{\partial q_2}{\partial y} - \frac{\partial q_2}{\partial x}\frac{\partial p_2}{\partial y}) &= a_{12}, \\
(\frac{\partial p_1}{\partial x}\frac{\partial q_1}{\partial z} - \frac{\partial q_1}{\partial x}\frac{\partial p_1}{\partial z}) + (\frac{\partial p_2}{\partial x}\frac{\partial q_2}{\partial z} - \frac{\partial q_2}{\partial x}\frac{\partial p_2}{\partial z}) &= a_{13}, \\
(\frac{\partial p_1}{\partial y}\frac{\partial q_1}{\partial z} - \frac{\partial q_1}{\partial y}\frac{\partial p_1}{\partial z}) + (\frac{\partial p_2}{\partial y}\frac{\partial q_2}{\partial z} - \frac{\partial q_2}{\partial y}\frac{\partial p_2}{\partial z}) &= a_{23}, \\
(\frac{\partial p_1}{\partial x}\frac{\partial q_1}{\partial u} - \frac{\partial q_1}{\partial x}\frac{\partial p_1}{\partial u}) + (\frac{\partial p_2}{\partial x}\frac{\partial q_2}{\partial u} - \frac{\partial q_2}{\partial x}\frac{\partial p_2}{\partial u}) &= -b_1, \\
(\frac{\partial p_1}{\partial y}\frac{\partial q_1}{\partial u} - \frac{\partial q_1}{\partial y}\frac{\partial p_1}{\partial u}) + (\frac{\partial p_2}{\partial y}\frac{\partial q_2}{\partial u} - \frac{\partial q_2}{\partial y}\frac{\partial p_2}{\partial u}) &= -b_2, \\
(\frac{\partial p_1}{\partial z}\frac{\partial q_1}{\partial u} - \frac{\partial q_1}{\partial z}\frac{\partial p_1}{\partial u}) + (\frac{\partial p_2}{\partial z}\frac{\partial q_2}{\partial u} - \frac{\partial q_2}{\partial z}\frac{\partial p_2}{\partial u}) &= -b_3.
\end{aligned} \tag{7}
$$

We reorganize Eq. (7) to a concise form and get the following theorem.

Theorem 1 *The canonical coordinates $\mathbf{Z} = (p_1,\ p_2,\ q_1,\ q_2)^\top$ for the gyrocenter dynamics satisfy the following equations:*

$$
\begin{cases}
\nabla p_1 \times \nabla q_1 + \nabla p_2 \times \nabla q_2 = \nabla \times \mathbf{A} + u \nabla \times \mathbf{b}, \\
\nabla p_1 \dfrac{\partial q_1}{\partial u} - \nabla q_1 \dfrac{\partial p_1}{\partial u} + \nabla p_2 \dfrac{\partial q_2}{\partial u} - \nabla q_2 \dfrac{\partial p_2}{\partial u} = -\mathbf{b},
\end{cases} \tag{8}
$$

where $\nabla = (\frac{\partial}{\partial x}, \frac{\partial}{\partial y}, \frac{\partial}{\partial z})^\top$, $\mathbf{A}$ is the vector potential and $\mathbf{b}$ is the unit vector along the direction of magnetic field in the gyrocenter dynamics.

The theorem offers an equivalent description for the canonical coordinates in the general sense, which enable us to obtain the canonical form of the gyrocenter system. Considering

the first equation of Eq. (8) is linear with respect to u, we expand the new coordinates p_1, p_2, q_1, q_2 in the series of u as

$$
\begin{aligned}
p_1(\mathbf{v}) &= p_{10}(\mathbf{X}) + \sum_{i=1}^{+\infty} u^i p_{1i}(\mathbf{X}), \\
p_2(\mathbf{v}) &= p_{20}(\mathbf{X}) + \sum_{i=1}^{+\infty} u^i p_{2i}(\mathbf{X}), \\
q_1(\mathbf{v}) &= q_{10}(\mathbf{X}) + \sum_{i=1}^{+\infty} u^i q_{1i}(\mathbf{X}), \\
q_2(\mathbf{v}) &= q_{20}(\mathbf{X}) + \sum_{i=1}^{+\infty} u^i q_{2i}(\mathbf{X}).
\end{aligned}
\tag{9}
$$

Submitting the expansion series to Eq. (8) and comparing the coefficients of u^k, we can obtain the equations for the coefficients,

$$
\nabla p_{10} \times \nabla q_{10} + \nabla p_{20} \times \nabla q_{20} = \nabla \times \mathbf{A}, \tag{10}
$$

$$
q_{11} \nabla p_{10} - p_{11} \nabla q_{10} + q_{21} \nabla p_{20} - p_{21} \nabla q_{20} = -\mathbf{b}, \tag{11}
$$

$$
\begin{aligned}
q_{1k} \nabla p_{10} - p_{1k} \nabla q_{10} &+ q_{2k} \nabla p_{20} - p_{2k} \nabla q_{20} = \\
-\frac{1}{k} \Bigg(\sum_{i=1}^{k-1} i q_{1i} \nabla p_{1,k-i} &- \sum_{i=1}^{k-1} i p_{1i} \nabla q_{1,k-i} \\
+ \sum_{i=1}^{k-1} i q_{2i} \nabla p_{2,k-i} &- \sum_{i=1}^{k-1} i p_{2i} \nabla q_{2,k-i} \Bigg).
\end{aligned}
\tag{12}
$$

The canonical coordinates are expressed in series form and can be calculated recursively. In the process of numerical calculation, only matrix multiplication, instead of solving differential equations, is involved.

To express the canonical coordinates in terms of the old gyrocenter coordinates, we need to use the expression of the magnetic field. Generally speaking, the vector potential $\mathbf{A}$ can be expressed in any coordinates $(\alpha,\ \beta,\ \gamma)$ as $\mathbf{A} = A_\alpha \nabla\alpha + A_\beta \nabla\beta + A_\gamma \nabla\gamma$. This formula can be transformed to another form

$$
\mathbf{A} = \nabla\eta + p_{10}\nabla q_{10} + p_{20}\nabla q_{20}, \tag{13}
$$

where $q_{10} = \beta$, $q_{20} = \gamma$, $\eta = \int^\alpha A_\alpha(\alpha',\beta,\gamma)d\alpha'$, $p_{10} = A_\beta - \partial\eta/\partial\beta$ and $p_{20} = A_\gamma - \partial\eta/\partial\gamma$. Then the formula Eq. (10) is satisfied automatically. Without loss of generality, ∇p_{10}, ∇p_{20}, ∇q_{20} can be taken to be linearly independent. Apparently, there are too

8

many freedoms to determine the coefficients of the series. Further restrictions should be applied. Setting $q_{2k} = 0$, for $k \geq 1$, we can get q_{11}, p_{11} and p_{21} from Eq. (11) using matrix multiplication

$$\begin{pmatrix} q_{11} \\ p_{11} \\ p_{21} \end{pmatrix} = (\nabla p_{10}, -\nabla q_{10}, -\nabla q_{20})^{-1}(-\mathbf{b}). \tag{14}$$

Then p_{1k}, q_{1k} and p_{2k}, for $k > 1$, can be obtained recursively from Eq. (12) in a similar manner. In this process, no solving of differential equations is involved, which is different from the standard proof of Darboux's theorem.

The canonical coordinates of gyrocenter dynamics are expressed by series of the parallel velocity u. To further study the property of the series, we can rewrite it as a series of a dimensionless variable ϵ. We define the dimensionless variable $\epsilon = \frac{mu}{qBL_B}$, where $L_B = \frac{B}{|\nabla B|}$ is the characteristic length of the magnetic field. The condition for the gyrocenter dynamics to be valid is $\epsilon \ll 1$. So the canonical coordinates can be expressed by series of a small variable ϵ depending only on the parallel velocity u,

$$\begin{aligned} p_1 = p_{10} + \sum_{i=1}^{\infty} \epsilon^i \widehat{p}_{1i}, \; p_2 = p_{20} + \sum_{i=1}^{\infty} \epsilon^i \widehat{p}_{2i}, \\ q_1 = q_{10} + \sum_{i=1}^{\infty} \epsilon^i \widehat{q}_{1i}, \; q_2 = q_{20} + \sum_{i=1}^{\infty} \epsilon^i \widehat{q}_{2i}. \end{aligned} \tag{15}$$

The truncation of the series at a given order is an asymptotic approximation to the exact canonical coordinates as $\epsilon \to 0$. Actually, the first order truncation, i.e., $\widetilde{p}_1 = p_{10} + \epsilon\widehat{p}_{11}$, $\widetilde{p}_2 = p_{20} + \epsilon\widehat{p}_{21}$, $\widetilde{q}_1 = q_{10} + \epsilon\widehat{q}_{11}$ and $\widetilde{q}_2 = q_{20}$, satisfies the following equations

$$\begin{aligned} \nabla\widetilde{p}_1 \times \nabla\widetilde{q}_1 + \nabla\widetilde{p}_2 \times \nabla\widetilde{q}_2 \\ =\mathbf{B} + u\nabla \times \mathbf{b} - \frac{\epsilon^2}{2}\nabla \times (\widehat{q}_{11}\nabla\widehat{p}_{11} - \widehat{p}_{11}\nabla\widehat{q}_{11}), \end{aligned} \tag{16}$$

$$\begin{aligned} \nabla\widetilde{p}_1\frac{\partial \widetilde{q}_1}{\partial u} - \nabla\widetilde{q}_1\frac{\partial \widetilde{p}_1}{\partial u} + \nabla\widetilde{p}_2\frac{\partial \widetilde{q}_2}{\partial u} - \nabla\widetilde{q}_2\frac{\partial \widetilde{p}_2}{\partial u} \\ = - \left[\mathbf{b} - \epsilon(\widehat{q}_{11}\nabla\widehat{p}_{11} - \widehat{p}_{11}\nabla\widehat{q}_{11})\right]. \end{aligned} \tag{17}$$

The truncation at the first-order leads to canonical coordinates for a gyrocenter system corresponding to an exact lagrangian L_1

$$L_1 = \left[\mathbf{A}(\mathbf{X}) + u\mathbf{b}(\mathbf{X}) - \frac{\epsilon^2}{2}(\widehat{q}_{11}\nabla\widehat{p}_{11} - \widehat{p}_{11}\nabla\widehat{q}_{11})\right] \cdot \dot{\mathbf{X}} - H(\mathbf{v}). \tag{18}$$

Similarly, the k-th order approximate canonical coordinates

$$\widetilde{p}_1 = \sum_{i=0}^{k} u^i p_{1i}, \ \widetilde{q}_1 = \sum_{i=0}^{k} u^i q_{1i}, \ \widetilde{p}_2 = \sum_{i=0}^{k} u^i p_{2i}, \ \widetilde{q}_2 = q_{20}, \tag{19}$$

satisfy

$$
\begin{aligned}
&\nabla \widetilde{p}_1 \frac{\partial \widetilde{q}_1}{\partial u} - \nabla \widetilde{q}_1 \frac{\partial \widetilde{p}_1}{\partial u} + \nabla \widetilde{p}_2 \frac{\partial \widetilde{q}_2}{\partial u} - \nabla \widetilde{q}_2 \frac{\partial \widetilde{p}_2}{\partial u} \\
&= \Big(\sum_{i=0}^{k} u^i \nabla p_{1i} \Big) \Big(\sum_{i=1}^{k} i u^{i-1} q_{1i} \Big) - \Big(\sum_{i=0}^{k} u^i \nabla q_{1i} \Big) \Big(\sum_{i=1}^{k} i u^{i-1} p_{1i} \Big) \\
&\quad + \Big(\sum_{i=0}^{k} u^i \nabla p_{2i} \Big) \Big(\sum_{i=1}^{k} i u^{i-1} q_{2i} \Big) - \Big(\sum_{i=0}^{k} u^i \nabla q_{2i} \Big) \Big(\sum_{i=1}^{k} i u^{i-1} p_{2i} \Big) \\
&= -\mathbf{b} + \sum_{l=1}^{k-1} u^l \Big[\Big(\sum_{m=1}^{l+1} m q_{1,m} \nabla p_{1,l+1-m} - m p_{1,m} \nabla q_{1,l+1-m} \\
&\quad + m q_{2,m} \nabla p_{2,l+1-m} - m p_{2,m} \nabla q_{2,l+1-m} \Big) \Big] + \mathcal{O}(u^k) \\
&= -\mathbf{b} + \mathcal{O}(u^k) = -\mathbf{b} + \mathcal{O}(\epsilon^k).
\end{aligned}
\tag{20}
$$

In Eq. (20), the third equality holds because $(q_{1i}, \ p_{1i}, \ p_{2i})$ are chosen to satisfy Eq. (12). On the other hand, $\widetilde{p}_1$, $\widetilde{q}_1$, $\widetilde{p}_2$ and $\widetilde{q}_2$ also satisfy

$$\nabla \widetilde{p}_1 \times \nabla \widetilde{q}_1 + \nabla \widetilde{p}_2 \times \nabla \widetilde{q}_2 = \mathbf{B} + u \nabla \times \mathbf{b} + \mathcal{O}(\epsilon^{k+1}). \tag{21}$$

We observe that the truncation at the k-order for canonical coordinates are the exact canonical coordinates for the gyrocenter system with the Lagrangian L_k

$$L_k = (\mathbf{A}(\mathbf{X}) + u\mathbf{b} + \mathcal{O}(\epsilon^{k+1}))\dot{\mathbf{X}} - H(\mathbf{v}), \tag{22}$$

which is k-order approximation to the original Lagrangian. The truncation of the series of the canonical coordinates as the exact canonical coordinates for the approximate Lagrangian is not only convenient in numerical simulations, but also has a physical meaning.

III. THE CANONICALIZATION OF GYROCENTERS IN MAGNETIC FIELDS WITH FLUX SURFACES

In this section, we give the canonicalization of gyrocenter systems in magnetic fields with flux surfaces. This kind of magnetic fields satisfies $B \cdot \nabla \Psi = 0$, where Ψ is the flux label. If

10

it can be written in two forms as

$$\begin{cases} \mathbf{B} = \nabla p_1 \times \nabla q_{10} + \nabla p_2 \times \nabla q_{20}, \\ \mathbf{B} = q_{11} \nabla p_1 + q_{21} \nabla p_2. \end{cases} \tag{23}$$

According to the theorem in Sec. II, because the magnetic field can be expressed in the above two forms, the recursive process for the coefficients of the series terminates at the second order. Then the canonical coordinates can be explicitly given as

$$\begin{aligned} p_1, \ q_1 &= q_{10} - \frac{u}{B(\mathbf{x})} q_{11}, \\ p_2, \ q_2 &= q_{20} - \frac{u}{B(\mathbf{x})} q_{21}, \end{aligned} \tag{24}$$

and the gyrocenter dynamics become canonical Hamiltonian system in the new coordinates. Previous work[20, 21] have also assumed the forms of magnetic field in Eq. (23).

In the following, we will describe why the magnetic field can be written in two forms as Eq. (23). Firstly, we find two functions $p_1(x, y, z)$ and $p_2(x, y, z)$ such that $\nabla p_1 \cdot \nabla \Psi = \nabla p_2 \cdot \nabla \Psi = 0$. Thus, $(p_1, \ p_2, \ \Psi)$ forms a well defined curvilinear coordinate system with the following properties

$$\begin{cases} \nabla p_1 \times \nabla p_2 = g_\Psi \nabla \Psi, \\ \nabla p_1 \times \nabla \Psi = f_1 \nabla p_1 + f_2 \nabla p_2, \\ \nabla p_2 \times \nabla \Psi = g_1 \nabla p_1 + g_2 \nabla p_2, \end{cases} \tag{25}$$

where f_1, f_2, g_1, g_2 and g_Ψ are related functions. In this flux surface coordinate system, the magnetic field $\mathbf{B}$ has the covariant representation:

$$\mathbf{B} = B_1 \nabla p_1 + B_2 \nabla p_2. \tag{26}$$

According to Eq. (25), we rewrite $\mathbf{B}$ as

$$\begin{aligned} \mathbf{B} &= \nabla p_1 \times \nabla F_1(p_1, \ p_2, \ \Psi) + \nabla p_2 \times \nabla F_2(p_1, \ p_2, \ \Psi) \\ &= \left(\frac{\partial F_1}{\partial \Psi} f_1 + \frac{\partial F_2}{\partial \Psi} g_1 \right) \nabla p_1 + \left(\frac{\partial F_1}{\partial \Psi} f_2 + \frac{\partial F_2}{\partial \Psi} g_2 \right) \nabla p_2 \\ &\quad + (\frac{\partial F_1}{\partial p_2} - \frac{\partial F_2}{\partial p_1}) g_\Psi \nabla \Psi. \end{aligned} \tag{27}$$

In general, the three directions ∇p_1, ∇p_2 and $\nabla \Psi$ are independent. So the functions F_1 and

11

F_2 should satisfy the following conditions

$$\begin{cases} \dfrac{\partial F_1}{\partial \Psi} f_1 + \dfrac{\partial F_2}{\partial \Psi} g_1 = B_1, \\ \dfrac{\partial F_1}{\partial \Psi} f_2 + \dfrac{\partial F_2}{\partial \Psi} g_2 = B_2, \\ \dfrac{\partial F_1}{\partial p_2} - \dfrac{\partial F_2}{\partial p_1} = 0. \end{cases} \tag{28}$$

To let F_1 and F_2 satisfy Eq. (28), we define

$$\begin{cases} F_1 = \displaystyle\int^\Psi \dfrac{B_1 g_2 - B_2 g_1}{g_2 f_1 - g_1 f_2} d\Psi', \\ F_2 = -\displaystyle\int^\Psi \dfrac{B_1 f_2 - B_2 f_1}{g_2 f_1 - g_1 f_2} d\Psi'. \end{cases} \tag{29}$$

According to the definition of Jacobian $J \equiv \nabla p_1 \cdot (\nabla p_2 \times \nabla \Psi)$ and Eq. (25), we get

$$\begin{aligned} &g_2 f_1 - g_1 f_2 \\ &= -\frac{J g_2}{\nabla p_1 \cdot \nabla p_2} = \frac{J g_1}{|\nabla p_2|^2} = \frac{J f_1}{\nabla p_1 \cdot \nabla p_2} = -\frac{J f_2}{|\nabla p_1|^2}. \end{aligned} \tag{30}$$

If $\nabla p_1 \cdot \nabla p_2 = 0$, Eq. (30) degenerates to $-g_1 f_2 = \frac{J g_1}{|\nabla p_2|^2}, = -\frac{J f_2}{|\nabla p_1|^2}$. We know that $g_2 f_1 - g_1 f_2 \neq 0$, which guarantees that F_1 and F_2 in Eq. (29) are meaningful. Obviously, F_1 and F_2 are well defined and automatically satisfy the first two equations in Eq. (28). Furthermore, using Eq. (30), we get

$$\begin{cases} \dfrac{\partial F_1}{\partial p_2} = -\dfrac{\partial}{\partial p_2} \displaystyle\int^\Psi \dfrac{\mathbf{B} \cdot \nabla p_2}{J} d\Psi', \\ \dfrac{\partial F_2}{\partial p_1} = \dfrac{\partial}{\partial p_1} \displaystyle\int^\Psi \dfrac{\mathbf{B} \cdot \nabla p_1}{J} d\Psi'. \end{cases} \tag{31}$$

It can be verified that Eq. (28) is equivalent to the divergence-free property of the magnetic field,

$$0 = \nabla \cdot \mathbf{B} = J \left[\frac{\partial}{\partial p_1} \left(\frac{\mathbf{B} \cdot \nabla p_1}{J} \right) + \frac{\partial}{\partial p_2} \left(\frac{\mathbf{B} \cdot \nabla p_2}{J} \right) \right]. \tag{32}$$

This is physically correct and self-consistent. Thus the canonical coordinates are

$$\begin{cases} p_1, \ q_1 = F_1 - \dfrac{u}{B} B_1, \\ p_2, \ q_2 = F_2 - \dfrac{u}{B} B_2, \end{cases} \tag{33}$$

where F_1 and F_2 are defined in Eq. (29). If ∇p_1 and ∇p_2 are orthogonal, the transformation also holds. Therefore exact canonical coordinates of the gyrocenter system in a magnetic with flux surfaces can be constructed and canonical symplectic simulation of gyrocenter dynamics can be performed without any approximation.

IV. THE CANONICAL SYMPLECTIC SIMULATION OF GYROCENTER DYNAMICS

With the effective canonicalization procedure for gyrocenter systems discussed in Secs. II and III, we explicitly constructed a transformation $\mathbf{Z} = \Phi(\mathbf{v})$ that brings non-canonical Hamiltonian system $\dot{\mathbf{v}} = K^{-1}(\mathbf{v})\nabla H(\mathbf{v})$ to the standard Hamiltonian system $\dot{\mathbf{Z}} = J^{-1}\nabla\widetilde{H}(\mathbf{Z})$. We now set foot in the canonical symplectic simulation of gyrocenter dynamics. The symplectic method is a well-known numerical integrator with appropriate global conservation properties for Hamiltonian systems with a canonical structure. This integrator conserves the canonical symplectic structure exactly and guarantees that the energy error is bounded by a small number for all the time steps[23–31]. According to the traditional procedure, the symplectic algorithm should be proceed as follows: (i) compute $\mathbf{Z}_n = \Phi(\mathbf{v}_n)$; (ii) apply a symplectic method to the standard system which yields $\mathbf{Z}_{n+1} = \psi_h(\mathbf{Z}_n)$; (iii) compute finally $\mathbf{v}_{n+1}$ from $\mathbf{Z}_{n+1} = \Phi(\mathbf{v}_{n+1})$.

One kind of convenient and useful symplectic methods is the symplectic Runge-Kutta method. A standard Runge-Kutta method can be expressed as

$$
\begin{cases}
\mathbf{Z}_{n+1} = \mathbf{Z}_n + h\sum_{i=1}^{s} b_i J^{-1}\nabla\widetilde{H}(K_i), \\
\quad K_i = \mathbf{Z}_n + h\sum_{j=1}^{s} a_{ij} J^{-1}\nabla\widetilde{H}(K_j).
\end{cases}
\tag{34}
$$

where K_i are intermediate variables. If the coefficients satisfy

$$
b_i a_{ij} + b_j a_{ji} = b_i b_j, \text{ for all } i, j,
\tag{35}
$$

the Runge-Kutta method is a symplectic method[25].

In the numerical method, the corresponding Hamiltonian function $\widetilde{H}$ should be expressed as $\widetilde{H}(\mathbf{Z}) = H(\mathbf{v})$, where $\widetilde{H} = H \circ \Phi^{-1}$. Generally speaking, it's difficult to express the inverse of this coordinate transformation and thus the new Hamiltonian in new coordinates. Here, to overcome the difficulty, we express the Hamiltonian function $\widetilde{H}(\mathbf{Z})$ and the term $J^{-1}\nabla\widetilde{H}(\mathbf{Z})$ in the original coordinates $\mathbf{v}$ as

$$
\widetilde{H}(\mathbf{Z}) = H(\mathbf{v}),
\tag{36}
$$

$$
J^{-1}\nabla\widetilde{H}(\mathbf{Z}) = (\frac{\partial\Phi}{\partial\mathbf{v}})K(\mathbf{v})^{-1}\nabla H(\mathbf{v}).
\tag{37}
$$

13

Equation (37) holds because of the chain rule

$$J^{-1}\nabla\widetilde{H}(\mathbf{Z}) = \dot{\mathbf{Z}} = \frac{\partial\Phi}{\partial\mathbf{v}}\dot{\mathbf{v}} = \left(\frac{\partial\Phi}{\partial\mathbf{v}}\right)K(\mathbf{v})^{-1}\nabla H(\mathbf{v}). \tag{38}$$

The fact that the coordinates transformation is reversible guarantees that for every K_i, there is a corresponding W_i, such that $J^{-1}\nabla\widetilde{H}(K_i) = \left(\frac{\partial\Phi}{\partial\mathbf{v}}\right)K(\mathbf{v})^{-1}\nabla H(\mathbf{v})\Big|_{\mathbf{v}=W_i}$. Then the symplectic simulation for the gyrocenter dynamics Eq. (34) can be rewritten as

$$\begin{cases} \Phi(\mathbf{v_{n+1}}) = \Phi(\mathbf{v_n}) + h\sum_{i=1}^{s} b_i\left(\frac{\partial\Phi}{\partial\mathbf{v}}\right)K(\mathbf{v})^{-1}\nabla H(\mathbf{v})\Big|_{\mathbf{v}=W_i}, \\ \Phi(W_i) = \Phi(\mathbf{v_n}) + h\sum_{j=1}^{s} a_{ij}\left(\frac{\partial\Phi}{\partial\mathbf{v}}\right)K(\mathbf{v})^{-1}\nabla H(\mathbf{v})\Big|_{\mathbf{v}=W_j}. \end{cases} \tag{39}$$

The iteration method is convenient for computing and the calculating of the gradient of the new Hamiltonian function $\widetilde{H}$ is avoided. Though the iteration is expressed normally in the original coordinates, it's essentially the symplectic simulation for the canonicalized gyrocenter dynamics in new coordinates, which means that symplectic simulation of the gyrocenter dynamics is realized. For example, when we apply the mid-point rule which is a symplectic and reversible method of order 2,

$$\mathbf{Z}_{n+1} = \mathbf{Z}_n + hJ^{-1}\nabla H\left(\frac{\mathbf{Z}_n + \mathbf{Z}_{n+1}}{2}\right), \tag{40}$$

to the transformed canonical Hamiltonian system, the following implicit iterations in the coordinate $\mathbf{v}_n$

$$\begin{cases} \Phi(\mathbf{v}_{n+1}) = \Phi(\mathbf{v}_n) + h\left(\frac{\partial\Phi}{\partial\mathbf{v}}\right)K(\mathbf{v})^{-1}\nabla H(\mathbf{v})\Big|_{\mathbf{v}=W}, \\ \Phi(W) = \Phi(\mathbf{v}_n) + \frac{1}{2}h\left(\frac{\partial\Phi}{\partial\mathbf{v}}\right)K(\mathbf{v})^{-1}\nabla H(\mathbf{v})\Big|_{\mathbf{v}=W}, \end{cases} \tag{41}$$

should be solved according to the above discussion.

In this canonical symplectic algorithm, numerical calculations are done directly using the original non-canonical coordinates. This involves multiplication by the Jacobian matrix. So rather than the expression of the canonical coordinates themselves, it is the Jacobian matrix that is needed. According to the procedure of the canonicalization, the canonical coordinates is expressed as a series in a small parameter linked to the parallel velocity. The zeroth order term can be readily computed from $\nabla \times \mathbf{A}$, and higher order terms can then be obtained by solving a linear system at each order. For example, to calculate p_{1i}, p_{2i}, q_{1i},

14

the gradients of p_{1j}, p_{2j}, q_{1j} $(0 \leq j \leq i-1)$ are required. In this process, the Jacobian matrix is automatically obtained as

$$\frac{\partial \Phi}{\partial \mathbf{v}} = \begin{pmatrix} \sum_{i=0}^{k} \nabla p_{1i} & \sum_{i=0}^{k} \nabla p_{2i} & \sum_{i=0}^{k} \nabla q_{1i} & \sum_{i=0}^{k} \nabla q_{2i} \\ \sum_{i=1}^{k} i p_{1i} u^{i-1} & \sum_{i=1}^{k} i p_{2i} u^{i-1} & \sum_{i=1}^{k} i q_{1i} u^{i-1} & \sum_{i=1}^{k} i q_{2i} u^{i-1} \end{pmatrix}^{T} \tag{42}$$

The advantage of this method is the avoidance of the back-and-forth transform of coordinates. So the inverse of the Jacobian matrix, which is usually difficult to calculate, is no longer required.

V. APPLICATION EXAMPLES

In this section, we give two application examples of our canonicalization method for the gyrocenter dynamics and apply symplectic method to the canonicalized Hamiltonian system. The numerical results demonstrate the superb properties of symplectic methods applied to the canonicalized gyrocenter equations in preserving the energy in long-time integration, compared to non-symplectic Runge-Kutta method applied directly to guiding-center equations itself.

A. Dipole magnetic field

For the gyrocenter dynamics in a dipole magnetic field, such as the earth magnetic field, we first give the canonical coordinates using canonicalization method discussed in Sec. II. Then the mid-point rule is applied to the canonical Hamiltonian system.

1. The canonical coordinates

The dipole magnetic field $\mathbf{B}$ is chosen to be

$$\mathbf{B}(\mathbf{X}) = (-M\frac{3xz}{r^5}, -M\frac{3yz}{r^5}, -M\frac{2z^2 - x^2 - y^2}{r^5}), \tag{43}$$

15

where $r = \sqrt{x^2 + y^2 + z^2}$ and M is a constant. The corresponding vector potential, the field strength $B(\mathbf{X})$ and unit magnetic field $\mathbf{b}(\mathbf{X})$ can be written as

$$\mathbf{A}(\mathbf{X}) = (\frac{My}{r^3}, -\frac{Mx}{r^3}, 0),$$
$$B(\mathbf{X}) = M\frac{r\sqrt{r^2 + 3z^2}}{r^5}, \tag{44}$$
$$\mathbf{b}(\mathbf{X}) = (-\frac{3xz}{r\sqrt{r^2 + 3z^2}}, -\frac{3yz}{r\sqrt{r^2 + 3z^2}}, -\frac{2z^2 - x^2 - y^2}{r\sqrt{r^2 + 3z^2}}).$$

Following the steps given in Sec. II, the vector potential can be written as

$$\mathbf{A} = M\frac{x^2 + y^2}{r^3}\nabla\arctan(\frac{x}{y}), \tag{45}$$

We set $p_{10} = M\frac{x^2 + y^2}{r^3}$, $q_{10} = \arctan(\frac{x}{y})$, $p10 = $ any function and $q_{20} = 0$. Then solving Eq. (11), we get $q_{11} = p_{11} = p_{21} = 0$ $p_{20} = -\frac{z}{r^3}$ and $q_{21} = \frac{r^4}{\sqrt{r^2+3z^2}}$. Because of $q_{11} = p_{11} = p_{21} = 0$, we don't need to solve Eq. (12) any more. The exact coordinates transformation is linear with respect to u and can be obtained as

$$p_1 = M\frac{x^2 + y^2}{r^3}, \ p_2 = -\frac{z}{r^3},$$
$$q_1 = \arctan(\frac{x}{y}), \ q_2 = u\frac{r^4}{\sqrt{r^2 + 3z^2}}. \tag{46}$$

The energy $H(\mathbf{v})$ is an invariant in original coordinates, and in new coordinates the Hamiltonian function $H(\mathbf{v}) = \widetilde{H}(\mathbf{Z})$ is also invariant. In numerical experiments, whether the energy error can be bounded is an important criterion.

2. The numerical results

For the gyrocenter dynamics in the dipole magnetic field, we first apply a non-symplectic implicit Runge-Kutta method of order 3 (RK3)

$$\begin{cases} \widetilde{\mathbf{v}}_{n+1} = \mathbf{v}_n + \frac{h}{2}J^{-1}\nabla H(K_1) + \frac{h}{2}J^{-1}\nabla H(K_2), \\ K_1 = \mathbf{v}_n + \frac{h}{2}J^{-1}\nabla H(K_1) - \frac{\sqrt{3}h}{6}J^{-1}\nabla H(K_2), \\ K_2 = \mathbf{v}_n + \frac{\sqrt{3}h}{6}J^{-1}\nabla H(K_1) + \frac{h}{2}J^{-1}\nabla H(K_2). \end{cases} \tag{47}$$

to the non-canonical Hamiltonian system to simulate particle's motion. Then we apply the mid-point rule which is a symplectic method of order 2 to the canonicalized gyrocenter
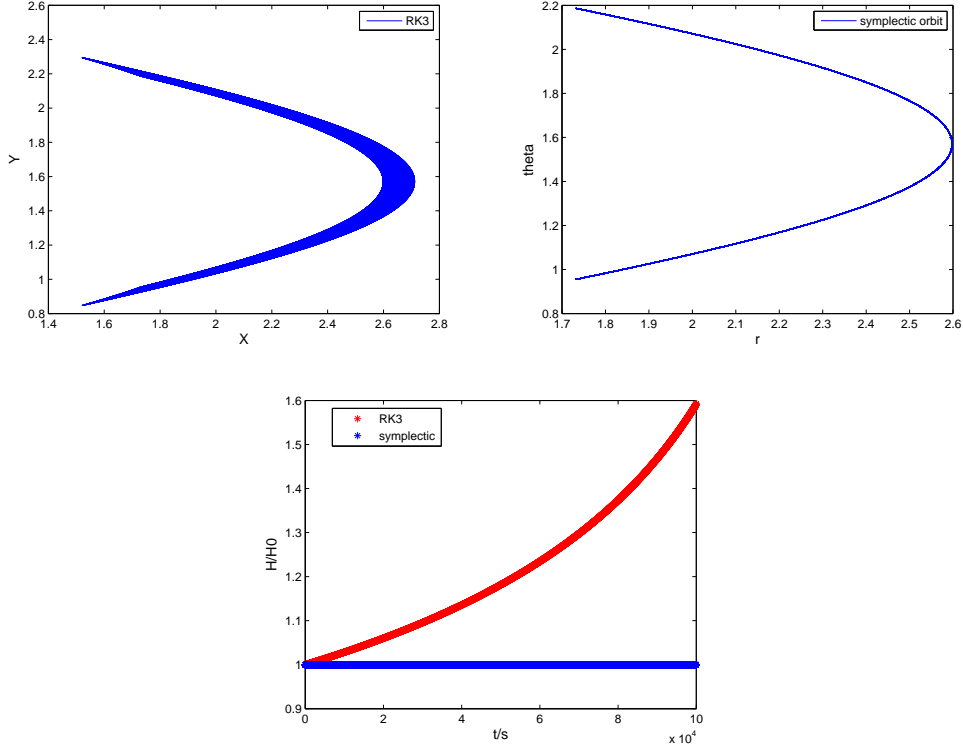
FIG. 1. Numerical results in a dipole field. [Fig. 1(a)] Orbit numerically obtained by using the standard RK3 method and [Fig. 1(b)] that obtained by the mid-point rule. [Fig. 1(c)] Normalized energy H/H0 as a function of time for both methods, where H0 is the initial energy. The time-step size is h=0.01≈ $T/100$. The integration time is 1000 periods of the orbit in the poloidal (azimuthal) plane.

equations. Displayed in Fig. (1) is the comparison of particle's orbit in dipole magnetic field calculated by the RK3 method and by mid-point rule with the same initial conditions. In these numerical examples, the parameters are chosen to be $M = 1000$ and $\mu = 0.01$. The initial conditions are $\mathbf{X}_0 = (1,1,1)$ and $u_0 = 0.01$. In Fig. 1(a), the orbit by RK3 applied to the gyro-center equations is not accurate, while the orbits calculated by mid-point rule applied to the canonicalized gyro-center equations in Fig. 1(b) is accurate over long integration time. Fig. 1(c) shows the evolution of the energy by the two methods and demonstrates the significant advantage of symplectic methods applied to the canonicalized Hamiltonian system in preserving energy for long-time integration.

17

B. The example in Tokamak magnetic configuration

For the gyrocenter dynamics in axisymmetric tokamak geometry, we give both the first-order approximate canonical coordinates and the exact canonical coordinates. Mid-point rule which is a symplectic method of order 2 is applied to canonicalized gyrocenter equations in both coordinates.

1. The canonical coordinates

Follow the procedure given in Sec. II, we can get the first-order approximate canonical transformation and the exact canonical coordinates for the guiding-center equations, so that we can apply symplectic methods to the canonicalized Hamiltonian system in new coordinates. In this geometry, there are two useful coordinate systems, the cylindrical coordinate system (R, ζ, z) and the toroidal coordinate system $(r, \theta, \overline{\zeta} = -\zeta)$. The magnetic field is chosen to be

$$\mathbf{B} = \frac{B_0 r}{qR} e_\theta + \frac{B_0 R_0}{R} e_\zeta = \frac{B_0 r^2}{qR} \nabla\theta - B_0 R_0 \nabla\zeta, \tag{48}$$

where B_0, R_0, q are constant with their usual meaning. The corresponding vector potential $\mathbf{A}$ can be written as

$$\mathbf{A} = \frac{B_0 r^2}{2Rq} e_\zeta - ln(\frac{R}{R_0})\frac{R_0 B_0}{2} e_z + \frac{B_0 R_0 z}{2R} e_R, \tag{49}$$

and the corresponding magnetic strength $B(\mathbf{x})$ and unit magnetic field $\mathbf{b}$ can be expressed as

$$B(\mathbf{x}) = \frac{B_0}{qR}\sqrt{r^2 + R_0^2 q^2},$$
$$\mathbf{b}(\mathbf{x}) = (\frac{-xz - R_0 qy}{R\sqrt{r^2 + R_0^2 q^2}}, \frac{-yz + R_0 qy}{R\sqrt{r^2 + R_0^2 q^2}}, \frac{R - R_0}{\sqrt{r^2 + R_0^2 q^2}}). \tag{50}$$

Following the steps in Sec. II, the vector potential is written as

$$\mathbf{A} = -\frac{B_0 r^2}{2q}\nabla\zeta - B_0 R_0 log(R)\nabla z + \nabla(\frac{B_0 R_0 z}{2} log(RR_0)), \tag{51}$$

where $\zeta = \arctan(\frac{x}{y})$. Setting $p_{10} = -B_0 R_0 log(R)$, $q_{10} = z$, $p_{20} = -\frac{B_0 r^2}{2q}$, $q_{20} = \zeta$, $q_{21} = 0$ and solving $q_{11}\nabla p_{10} - p_{11}\nabla q_{10} - p_{21}\nabla q_{20} = -\mathbf{b}$, we obtain the first-order approximate

18

canonical coordinates

$$
\begin{cases}
\widetilde{p}_1 = -B_0 R_0 log(R) + u \dfrac{R - R_0}{\sqrt{r^2 + R_0^2 q^2}}, \\[4mm]
\widetilde{p}_2 = -\dfrac{B_0 r^2}{2q} - u \dfrac{q R_0 R}{\sqrt{r^2 + R_0^2 q^2}}, \\[4mm]
\widetilde{q}_1 = z - u \dfrac{Rz}{R_0 R_0 \sqrt{r^2 + R_0^2 q^2}}, \\[4mm]
\widetilde{q}_2 = \arctan(\dfrac{x}{y}).
\end{cases}
\tag{52}
$$

The approximate canonical coordinates is easily obtained without the need to numerical solving. The canonical coordinates are not unique, another approximate canonical coordinates are

$$
\begin{cases}
\widetilde{p}_1 = 2z \sqrt{-B_0 R_0 \dfrac{R_0 log(R) - R + R_0}{(R - R_0)^2}} \\[4mm]
\quad - u \dfrac{z}{\sqrt{r^2 + R_0^2 q^2}} \sqrt{-\dfrac{1}{B_0 R_0} \dfrac{(R - R_0)^2}{R_0 log(R) - R + R_0}}, \\[4mm]
\widetilde{p}_2 = -\dfrac{B_0 r^2}{2q} - u \dfrac{q R_0 R}{\sqrt{r^2 + R_0^2 q^2}}, \\[4mm]
\widetilde{q}_1 = (R - R_0) \sqrt{-B_0 R_0 \dfrac{R_0 log(R) - R + R_0}{(R - R_0)^2}} \\[4mm]
\quad - u \dfrac{(R - R_0)}{2\sqrt{r^2 + R_0^2 q^2}} \sqrt{-\dfrac{1}{B_0 R_0} \dfrac{(R - R_0)^2}{R_0 log(R) - R + R_0}}, \\[4mm]
\widetilde{q}_2 = \arctan(\dfrac{x}{y}).
\end{cases}
\tag{53}
$$

Following Sec. II, we obtain the exact canonical coordinates

$$
\begin{cases}
p_1 = 2z \sqrt{-\dfrac{u}{\sqrt{r^2 + R_0^2 q^2}} - B_0 R_0 \dfrac{R_0 log(R) - R + R_0}{(R - R_0)^2}}, \\[4mm]
p_2 = -\dfrac{B_0 r^2}{2q} - u \dfrac{q R_0 R}{\sqrt{r^2 + R_0^2 q^2}}, \\[4mm]
q_1 = (R - R_0) \sqrt{-\dfrac{u}{\sqrt{r^2 + R_0^2 q^2}} - B_0 R_0 \dfrac{R_0 log(R) - R + R_0}{(R - R_0)^2}}, \\[4mm]
q_2 = \arctan(\dfrac{x}{y}).
\end{cases}
\tag{54}
$$

The transformation transforms the gyrocenter motion into a canonical Hamiltonian system $\dot{\mathbf{Z}} = J^{-1} \nabla \widetilde{H}(\mathbf{Z})$.

We first use the non-symplectic implicit Runge-Kutta method of order 3 to simulate the motion of charged particles, and then apply the mid-point rule to solve the gyrocenter equations in first-order approximate canonical coordinates and the exact canonical coordinates. We denote by ACT+S the method of symplectic method applied to guiding-center equations in first-order approximate canonical coordinates and by ECT+S the method of symplectic method applied to guiding-center equations in the exact canonical coordinates.

In these numerical examples, the parameters for the model tokamak geometry and simulation particles are normalized by R_0 and B_0 with safety factor $q = 2$. Displayed in Fig. (2) is the comparison of banana orbits calculated by the RK3 method, by the ECT+S method and by the ACT+S method with the same initial conditions. In these numerical examples, $\mu = 2.25 \times 10^{-6}$ and the initial conditions are $\mathbf{X}_0 = (1.05, 0, 0)$ and $u_0 = 0.0004306$. In Fig. 2(a), the orbit by RK3 is not accurate at the long time scale, while the orbits calculated by ECT+S method in Fig. 2(b) and that by 1-order ACT+S method in Fig. 2(c) are both accurate over long integration time and form closed banana orbits. Displayed in Fig. (3) is the comparison of a transit orbit calculated by the three methods with the same initial conditions. In this calculation, $\mu = 2.448 \times 10^{-6}$, and the initial conditions are $\mathbf{x}_0 = (1.05, 0, 0)$ and $u_0 = 0.0008117$. In Fig. 3(a), the orbit by RK3 is not accurate at the long time scale, while the orbits calculated by ECT+S in Fig. 3(b) and by ACT+S in Fig. 3(c) are both accurate over long integration time and forms a closed transit orbits.

The long-term energy by RK3 method gradually decreases without bound. However, for the symplectic integrator applied to canonical Hamiltonian system either in the approximate coordinates or in the exact canonical coordinates, the energy error is bounded by a small number for all time steps. This fact is clearly demonstrated in Fig. 2(d) and Fig. 3(d), where charged particle's energy normalized by the initial energy is plotted against time. In fact, the curve of discrete energy obtained by the mid-point rule in approximate canonical coordinates overlap the curve got in exact canonical coordinates. The numerical results clearly show that the symplectic integrator bounds globally the numerical energy error and maintains the accuracy of the orbit for arbitrarily long simulation time. In these numerical examples, for each time step of the symplectic method, five Newton iterations are used to search for the root. Though mid-point rule is of order 2, its numerical results show the
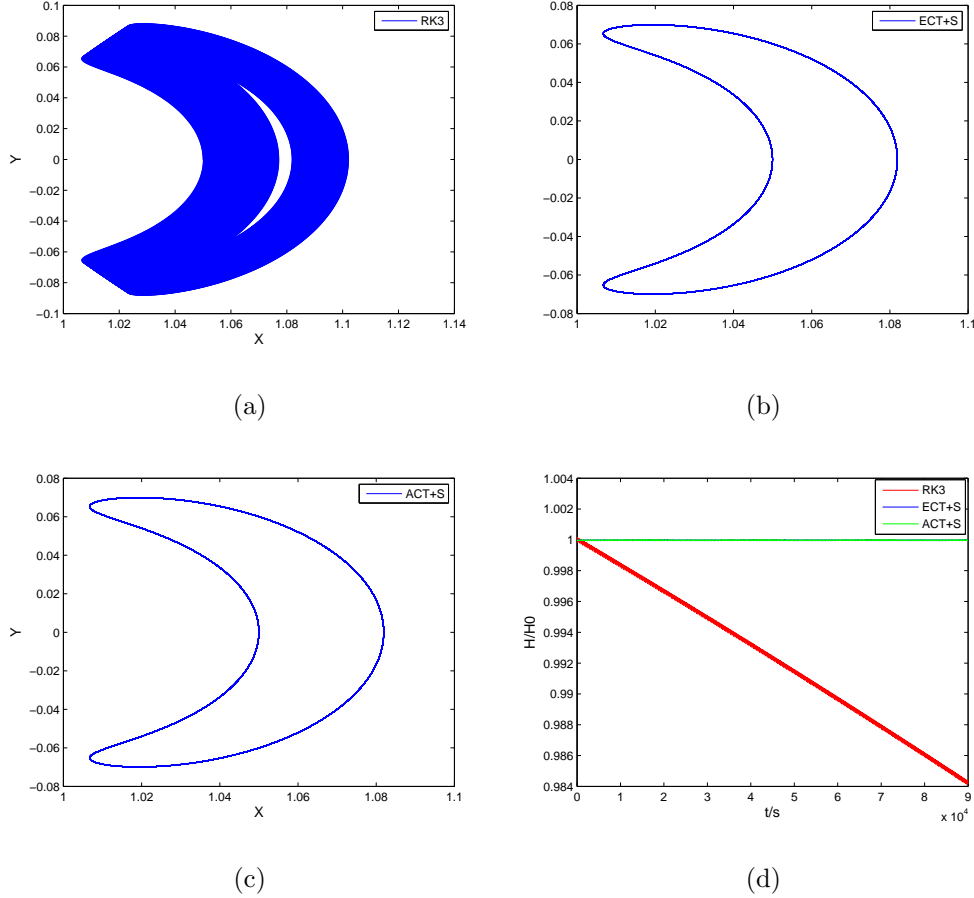
FIG. 2. (Color online) [Fig. 2(a)] Banana orbit numerically obtained by using the standard RK3 method and [Fig. 2(b)] that obtained by the ECT+S method. Fig. 2(c) is the orbit by the ACT+S method. The integration time is 250 periods of the closed orbit in the poloidal (azimuthal) plane. [Fig. 2(d)] Normalized energy H/H0 as a function of time for the three methods, where H0 is the initial energy. The time-step size is h=100$\approx T/400$.

superb properties for the guiding-center equation in the new coordinates than that of the standard RK3 method in long-time simulation. The results displayed in the Fig. (2) and Fig. (3) therefore provide an appropriate comparison in maintaining the accuracy of the orbit and in conserving energy.

VI. CONCLUSION

In this paper, we have developed a general procedure to construct canonical coordinates of the guiding center dynamics in time-independent magnetic fields. A series expansion of
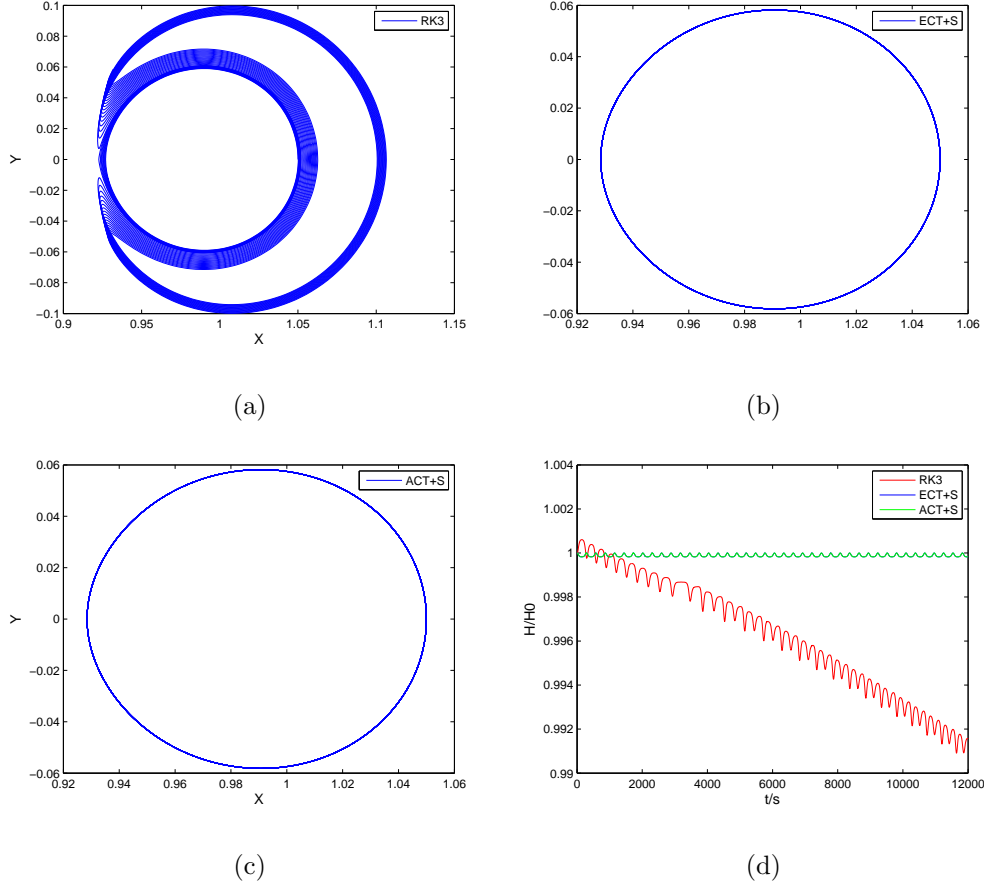
FIG. 3. (Color online) [Fig. 3(a)] Transit orbit numerically obtained by using the standard RK3 method and [Fig. 3(b)] that obtained by the ECT+S method. Fig. 3(c) is the transit orbit obtained by the ACT+S method. The integration time is 40 periods of the closed orbit in the poloidal (azimuthal) plane. [Fig. 3(d)] Normalized energy H/H0 as a function of time for three methods, where H0 is the initial energy. The time-step size is h=100 ≈ $T/300$.

the coordinates transformation is obtained recursively, and in numerical simulations we can use approximate canonical coordinates by truncating high order terms to a certain accuracy, such as the machine accuracy. We applied symplectic methods to the canonicalized gyro-center system in the original coordinates associated with the transformation. The examples in dipole magnetic field and in axisymmetric tokamak magnetic field demonstrated the significant advantages of symplectic method applied to the canonicalized system in preserving energy in long-term integration. The canonization method developed in this paper can be easily applied in numerical experiments.

The paper focus only on the guiding-center motion in a equilibrium field. For the guiding

center motion in a time-dependent electromagnetic field, the corresponding Lagrangian will depend on time explicitly, i.e., $L = L(\mathbf{X}, \dot{\mathbf{X}}, u, \dot{u}, t)$. In this case, the expression of the Euler-Lagrange equation are unchanged, and the system is still 4-dimensional. But the equations are time-dependent. We can extend the gyrocenter system to 6-dimensional and investigate its canonical coordinates in the similar way. The canonical transformation and the numerical properties in comparison with standard integrators will be investigated in future studies.

VII. ACKNOWLEDGEMENTS

[1] R. G. Littlejohn, J. Math. Phys. **20**, 2445 (1979).

[2] R. G. Littlejohn, J. Plasma Phys. **29**, 111 (1983).

[3] H. Qin, W. M. Tang, W. W. Lee, and G. Rewoldt, Phys. Plasmas **6**, 1575 (1999).

[4] A. J. Brizard, J. Plasma Phys. **41**, 541 (1989).

[5] A. J. Brizard, Phys. Fluids B **1**, 1381 (1989).

[6] J. C. Cummings, Ph.D. dissertation, (Princeton University) 1995.

[7] A. M. Dimits, T. J. Williams, J. A. Byers, and B. I. Cohen, Phys. Rev. Lett. **77**, 71 (1996).

[8] W. W. Lee, Phys. Fluids **26**, 556 (1983).

[9] W. W. Lee, J. Comput. Phys. **72**, 243 (1987).

[10] W. W. Lee and W. M. Tang, Phys. Fluids **31**, 612 (1988).

[11] Z. Lin, T. S. Hahm, W. W. Lee, W. M. Tang, and R.B. White, Science **281**, 1835 (1998).

[12] S. E. Parker, W. W. Lee, and R. A. Santoro, Phys. Rev. Lett. **71**, 2042 (1993).

[13] H. Qin, W. M. Tang, and G. Rewoldt, Phys. Plasmas **5**, 1035 (1998).

[14] H. Qin, Ph.D. dissertation, (Princeton University) 1998.

[15] R. D. Sydora, V. K. Decyk, and J. M. Dawson, Plasma Phys. Controlled Fusion **38**, A281 (1996).

[16] J. Y. Xiao, J. Liu, H. Qin, and Z. Yu, Phys. Plasmas **20**, 102517 (2013).

[17] J. X. Li, H. Qin, Z. Y. Pu, L. Xie, and S.Y. Fu, Phys. Plasmas **18**, 052902 (2011).

[18] H. Qin and X. Guan, *Phys. Rev. Lett.* **100**, 035006 (2008).

[19] H. Qin, X. Guan, and W. M. Tang, Phys. Plasmas **16**, 042510 (2009).

[20] J. D. Meiss and R. D. Hazeltine, Phys. Fluids B **2**, 2563 (1990).

[21] R. White and L. E. Zakharov, Phys. Plasmas **10**, 573 (2003).

[22] H. Gao, J. Yu, J. Nie, J. Yang, G. Wang, S. Yin, W. Liu, D. Wang, and P. Duan, Phys. Scr. **86** 065502 (2012).

[23] K. Feng, in *Proceedings of 1984 Beijing Symposium on Differential Geometry and Differential Equations*, edited by K. Feng (Science Press, Beijing, 1985), pp. 42-58.

[24] K. Feng, J. Comput. Math. **4**, 279 (1986).

[25] J. M. Sanz-Serna, BIT **28**, 877 (1988).

[26] P. J. Channell and C. Scovel, Nonlinearity **3**, 231 (1990).

[27] E. Forest and R. D. Ruth, Physica D **43**, 105 (1990).

[28] J. M. Sanz-Serna and M. P. Calvo, *Numerical Hamiltonian Problems*, Chapman and Hall, London, 1994.

[29] K. Feng, *Collected Works of Feng Kang (II)*, National Defence Industry Press, Beijing, 1995.

[30] E. Hairer, Ch. Lubich, and G. Wanner, *Geometric Numerical Integration: Structure-Preserving Algorithms for Ordinary Differential Equations*, Springer, 2002.

[31] K. Feng and M. Z. Qin, *Symplectic Geometric Algorithms for Hamiltonian System*, Springer, New York, 2009.